Electronic Supplementary Material (ESI) for Journal of Materials Chemistry A.

Supporting Information

Bi^{3+} Doped 2D Ruddlesden-Popper Organolead Iodide Perovskites

Feiyi Lyu,[a,b,c] Xiaoqi Zheng,[a] Yingqiao Wang,[a] Ruowen Shi,[a] Jianli Yang,[a] Ziyue Li,[a] Jiase Yu,[a] Bo-Lin Lin[a,b,c*]

[a] School of Physical Science and Technology, ShanghaiTech University, Shanghai 201210, China.

[b] Shanghai Institute of Ceramics, Chinese Academy of Sciences, Shanghai 200050, China.

[c] University of Chinese Academy of Sciences, Beijing 100049, China.

*Corresponding: E-mail: linbl@shanghaitech.edu.cn (Prof. B.-L. Lin). Tel: 86-021-206850

Table of Contents

1. Experimental Section **3**
1.1 Chemicals and Materials 3
1.2 Synthesis of undoped and doped 2D perovskite crystals 3
2. Characterization **5**
2.1 Powder X-ray Diffraction 5
2.2 Inductively Coupled Plasma-optical Emission Spectrometer 5
2.3 UV-vis Absorption 5
2.3 UV-vis Absorption 5
2.4 Fluorescence imaging 5
2.5 Photoluminescence 5
2.6 Time-resolved photoluminescence 5
2.7 Photostability measurement 5
2.8 DFT Calculations 5
3. Supporting Data **7**
3.1 Picture of crystal samples 7
3.2 XRD pattern of the samples 8
3.3 ICP-OES results 10
3.4 UV-vis absorption spectra of the samples 11
3.5 PL spectra of the samples 12
3.6 Lifetimes of the samples 13
3.7 Calculation results 18
3.8 XRD pattern for environment stability experiment 21
3.9 UV-vis absorption and PL spectra for doped samples 22
3.10 Photostability tests 23
3.11 PL spectra for unexfoliated samples 24
3.12 PL spectra for 4L samples 25
4. References **26**

Experimental Section

Chemicals and Materials

Hydriodic acid (HI, 55.0-58.0% w/w in water), Lead oxide (PbO, 99.97%) and Bismuth iodide (BiI_3, 99.99%) were purchased from Aladdin. Methylamine solution (CH_3NH_2, 27.0-32.0% w/w in alcohol) and n-Butylamine (n-$CH_3(CH_2)_3NH_2$) were purchased from Sinopharm. Hypophoaphoeous acid (H_3PO_2) 50% w/w in water) was purchased from Macklin. All chemicals are used as received.

Methylammonium iodide (MAI) was synthesized by neutralizing equimolar amounts of hydriodic acid solution (HI, 55.0-58.0% w/w in water) and methylamine solution (CH_3NH_2, 27.0-32.0% w/w in alcohol) in ice water bath for 2 hours. The white precipitation was collected after rotary evaporation at 60℃ and vacuum filtration, which was purified by ensuing dissolution using ethanol as solvent and precipitation using dimethyl ether as anti-solvent for three times. The white MAI powder was then vacuum drying at 60℃ for 24 hours.

Synthesis of undoped and doped 2D perovskite crystals. (the synthesis method was based on reference [1])

1L crystals:

PbO powder (669.6mg, 3 mmol) was dissolved in a mixture solution of 55-58% w/w aqueous HI (3.5 mL, 26.6mmol) and 50% w/w aqueous H_3PO_2 (0.6 mL, 5.47mmol) by heating to 85℃ under constant magnetic stirring about 15 min. For the doped samples, the required amount of bismuth iodide (BiI_3) was added to the solution. In a separate beaker, n-$CH_3(CH_2)_3NH_2$ (277μL, 3mmol) was neutralized with HI 55-58% w/w (1ml, 7.6mmol) in an ice bath resulting in a clear -yellow solution. Added the n-$CH_3(CH_2)_3NH_3I$ solution into the former solution and an orange precipitate would appear, which was subsequently dissolved under heating the combined solution at 85℃. The stirring was then stopped and the solution was slowly cooling to room temperature.

2L crystals

PbO powder (669.6mg, 3 mmol) was dissolved in a mixture solution of 55-58% w/w aqueous HI (3.5 mL, 26.6mmol) and 50% w/w aqueous H_3PO_2 (0.6 mL, 5.47mmol) by heating to 85℃ under constant magnetic stirring about 15 min. For the doped samples, the required amount of bismuth iodide (BiI_3) was added to the solution. Subsequent addition of solid CH_3NH_3I (238mg, 1.5mmol) to the solution initially caused the precipitation of a black powder, which were dissolved under stirring. In a separate beaker, n-$CH_3(CH_2)_3NH_2$ (208μL, 2.1mmol) was neutralized with HI 55-58% w/w (1ml, 7.6mmol) in an ice bath resulting in a clear pale-yellow solution. Added the n-$CH_3(CH_2)_3NH_3I$ solution into the former solution and a fuchsia precipitate would appear, which was subsequently dissolved under heating the combined solution at 85℃. The stirring was then stopped and the solution was slowly cooling to room temperature.

3L crystals

PbO powder (669.6mg, 3 mmol) was dissolved in a mixture solution of 55-58% w/w aqueous HI (3.5 mL, 26.6mmol) and 50% w/w aqueous H_3PO_2 (0.6 mL, 5.47mmol) by heating to 85℃ under constant magnetic stirring about 15 min. For the doped samples, the required amount of bismuth iodide (BiI_3) was added to the solution. Subsequent addition of solid CH_3NH_3I (317mg, 2mmol) to the solution initially caused the precipitation of a black powder, which are dissolved under stirring. In a separate beaker, n-$CH_3(CH_2)_3NH_2$ (98μL, 1mmol) was neutralized with HI 55-58% w/w (1ml, 7.6mmol) in an ice bath resulting in a clear pale-yellow solution. Added the n-$CH_3(CH_2)_3NH_3I$ solution into the former solution and a black precipitate would appear, which was subsequently dissolved under heating the combined solution at 85℃. The stirring was then stopped and the solution was slowly cooling to room temperature.

4L crystals

PbO powder (669.6mg, 3 mmol) was dissolved in a mixture solution of 55-58% w/w aqueous HI (3.5 mL, 26.6mmol) and 50% w/w aqueous H_3PO_2 (0.6 mL, 5.47mmol) by heating to 85℃ under constant magnetic stirring about 15 min. For the doped samples, the required amount of bismuth iodide (BiI_3) was added to the solution. Subsequent addition of solid CH_3NH_3I (357mg, 2.25mmol) to the solution initially caused the precipitation of a black powder, which are dissolved under stirring. In a separate beaker, n-$CH_3(CH_2)_3NH_2$ (75μL, 0.75mmol) was neutralized with HI 55-58% w/w (1ml, 7.6mmol) in an ice bath resulting in a clear pale-yellow solution. Added the n-$CH_3(CH_2)_3NH_3I$ solution into the former solution and a black precipitate would appear, which was subsequently dissolved under heating the combined solution at 85℃. The stirring was then stopped and the solution was slowly cooling to room temperature.

Characterization

Powder X-ray Diffraction (PXRD)

XRD patterns were acquired on a Bruker AXS D8 diffractometer using Cu-Kα radiation (λ=1.54178 Å). The temperature at the sample stage was ~300 K and was not regulated. Samples were manually pulverized using agate pestle and mortar.

Inductively Coupled Plasma-optical Emission Spectrometer (ICP-OES)

ICP test was performed on Thermo ICP-OES iCAP 7400 Radial. The pulverized sample was digested by aqua regia, then the solution was diluted with ultrapure water.

UV-vis Absorption

Room-temperature UV-vis diffusion reflectance spectra were measured on a Cary 5000 UV-vis-NIR spectrophotometer at λ = 400–900 nm coupled with an integrating sphere by using $BaSO_4$ powder as the reflectance reference.

Photoluminescence (PL)

The steady-state PL spectra were collected on oriented crystals on a Horiba Flourolog-3 spectrometer with a standard 450W Xenon CW lamp. The crystals were excited at 400nm.

Fluorescence imaging

The fluorescence imaging of the exfoliated crystals was performed on a Olympus XI83 Fluorescence microscope. The Bright field channel, Cy2 channel and Cy3 channel were used here. For Cy2 channel, the wavelength rang of excitation light is 450nm-490nm, the excitation peak is 470nm, this channel can collect the signal from 500nm-550nm. For Cy3 channel, the wavelength rang of excitation light is 532.5-557.5nm, the excitation peak is 545nm, this channel can collect the signal from 570nm-640nm.

Time-resolved photoluminescence (TRPL)

The TRPL spectra of the Excitonic PL was measured on a single-photon detector and counter (hydraharp 400, PicoQuant) which was used to detect and record the damped number of photons over time. The crystal samples were pulsed at 400nm. The 400nm pulsed excitation lasing was reached by a frequency-doubled mode-locked Ti-sapphire oscillator laser (800nm, 80MHz, 150fs, Coherent Inc) through a BBO crystal. The excitation intensity was typically maintained below 100 mW/cm^2 to prevent degradation. The crystal samples were exfoliated to get a fresh surface before the measurement.

Photostability measurement

A Charge Coupled Detector (CCD) was used to observe the image of the microstructure and fluorescence. The reflected PL emission signal was collected by the same microscope objective and analyzed by the spectrograph (IHR550, HORIBA), the excitation light source is the same as TRPL.

DFT Calculations

The doped $(BA)_2PbI_4$ (1L) structure was created by substituting a lead atom by a bismuth atom and eliminating a BA molecular in a 2×1×1 supercell (the experimental unit cell parameters a, b and c respectively of 8.8764, 8.86925 and 27.6014 Å)[2], which contains 7 lead atoms and 1 bismuth atom (295 atoms in total).

For $(BA)_2(MA)_2Pb_3I_{10}$ (3L) Bi-doped structures, two examples were created. A lead atom was replaced and a vacancy of MA was added between two different Pb-I layers in a 2×1×1 supercell (the unit cell parameters a, b and c respectively of 8.9275, 51.9590 and 8.8777 Å)[1], which contains 23 lead atoms and 1 bismuth atom (487 atoms in total).

The structure optimized, density of state (DOS) and partial charge calculation were used density function theory (DFT) as implanted in

Vienna ab initio Simulation Package (VASP)[3]. Perdew-Burke-Ernzerhof (PBE) exchange-correlation function[4] was used. The interaction of electrons and ions were described by ultrasoft pseudopotentials with electrons from H (1s), C (2s, 2p), N (2s, 2p), I (5s, 5p), Pb (5d, 6s,6p), Bi (5d, 6s, 6p). The plane-wave cut off energy was 400 eV, and the systems are relaxed until the energy change less than 1×10^{-4} eV. Γ point was chosen to be calculated. To properly take into account the long-range van der Waals interaction that plays a non-ignorable role in the hybrid perovskites involving organic molecules, the vdWs-optB86b functional[5] is adopted.

We also build a 2×2×1 supercell 1L system with a lead atom was replaced by a bismuth atom and a vacancy of BA, which contains 15 lead atoms and 1 bismuth atom (607 atoms in total). The DOS and partial charge plot are shown in Figure S12, which are consistent with the calculation results of 1L-2×1×1 system.

Supporting Data

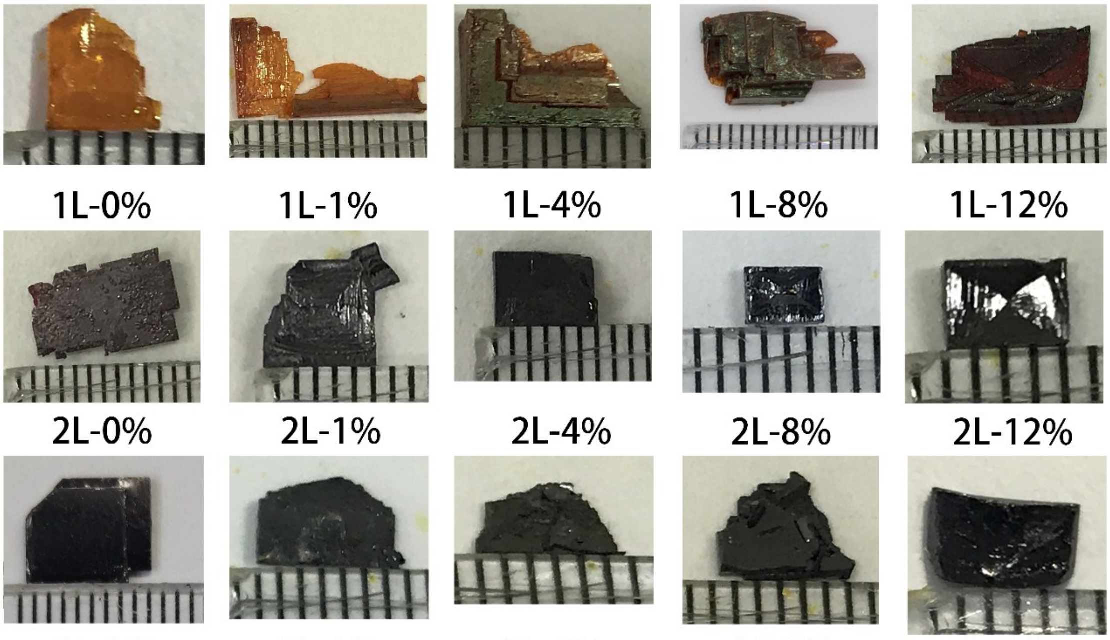
1L-0%
1L-1%
1L-4%
1L-8%
1L-12%
2L-0%
2L-1%
2L-4%
2L-8%
2L-12%
3L-0%
3L-1%
3L-4%
3L-8%
3L-12%

Figure S1. Pictures of 2D $(BA)_2(MA)_{n-1}Pb_nI_{3n+1}$ crystals having various Bi concentration in feed solutions for n=1, 2 & 3.

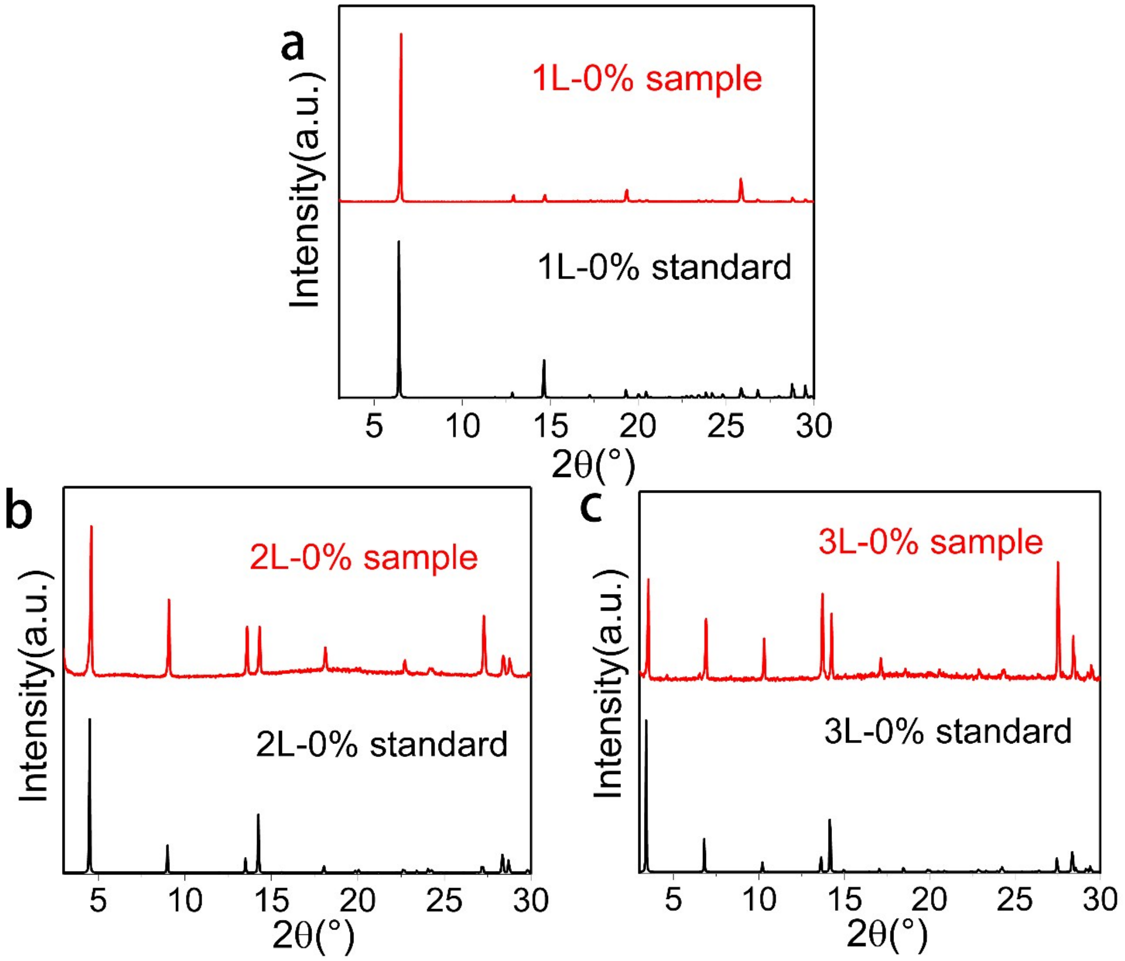

Figure S2. XRD pattern of undoped 2D perovskites and standard XRD for (a) 1L, (b) 2L & (c) 3L samples.

*The standard powder XRD are calculated based on their corresponding crystal structure data [1,2].

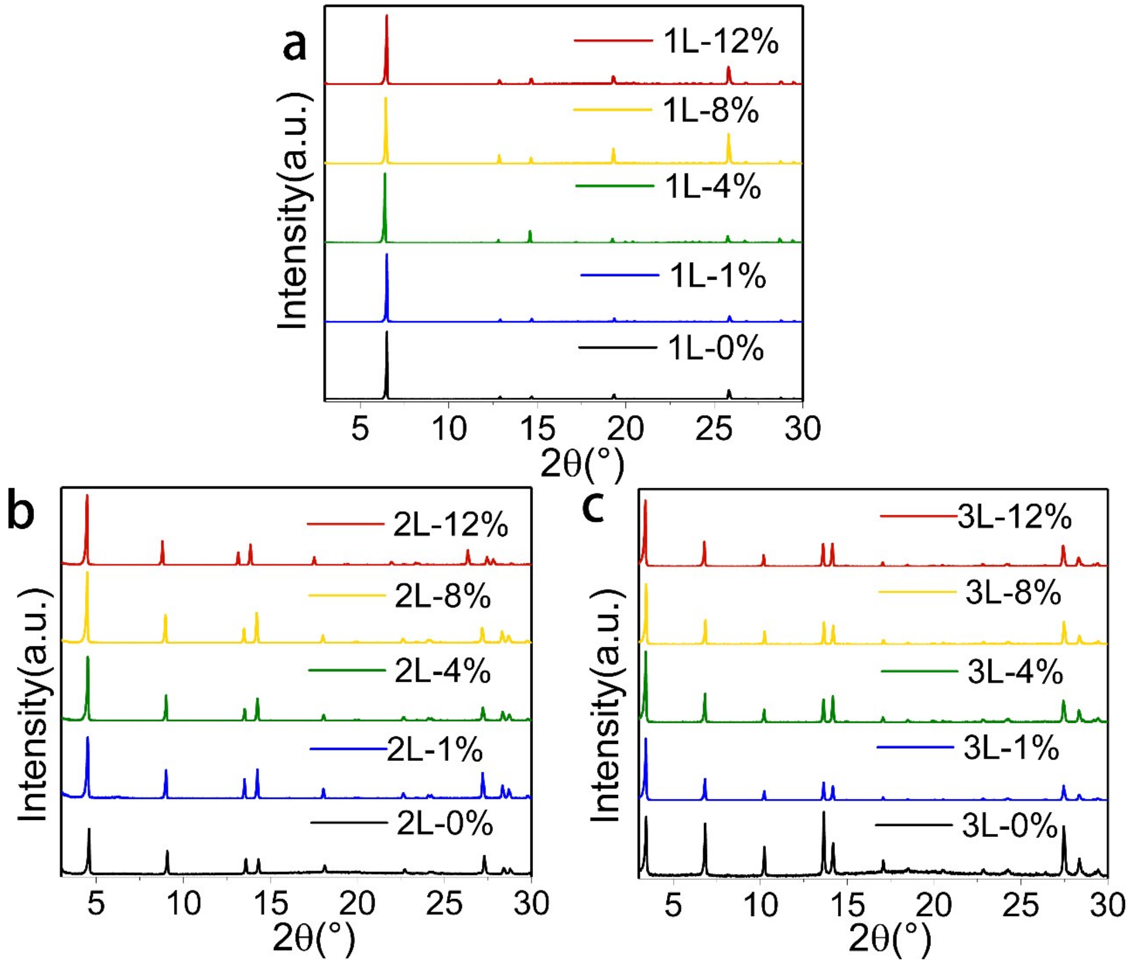

Figure S3. XRD pattern of 2D perovskite crystals with various Bi concentration in feed solutions for (a) 1L, (b) 2L & (c) 3L samples.

Table S1. Bi concentration in the feed solution and crystals

Bi% in feed solution	Bi% in 1L crystals	Bi% in 2L crystals	Bi% in 3L crystals
0	—	—	—
1	0.0294 ± 0.0076	0.0946 ± 0.0068	0.1847 ± 0.0099
4	0.1563 ±0.0044	0.2672 ± 0.0077	0.5304 ± 0.0042
8	0.3011 ± 0.0075	0.3688 ± 0.0055	0.7297 ± 0.0044
12	0.4491 ± 0.0036	0.5516 ± 0.0037	0.9974 ± 0.0020

Table S2. Bi concentration in the edge and center of the same Bi-doped crystals for 1L samples

Bi% in feed solution	Bi% in the edge of the crystal	Bi% in the center of the crystal	Bi%-edge/Bi%-center
0	—	—	
1	0.0434 ± 0.0039	0.0259 ± 0.0031	1.6757
4	0.2215 ± 0.0014	0.1399 ± 0.0005	1.5833
8	0.3192 ± 0.0022	0.2516 ± 0.0018	1.2687
12	0.5410 ± 0.0011	0.4805 ± 0.0048	1.1259

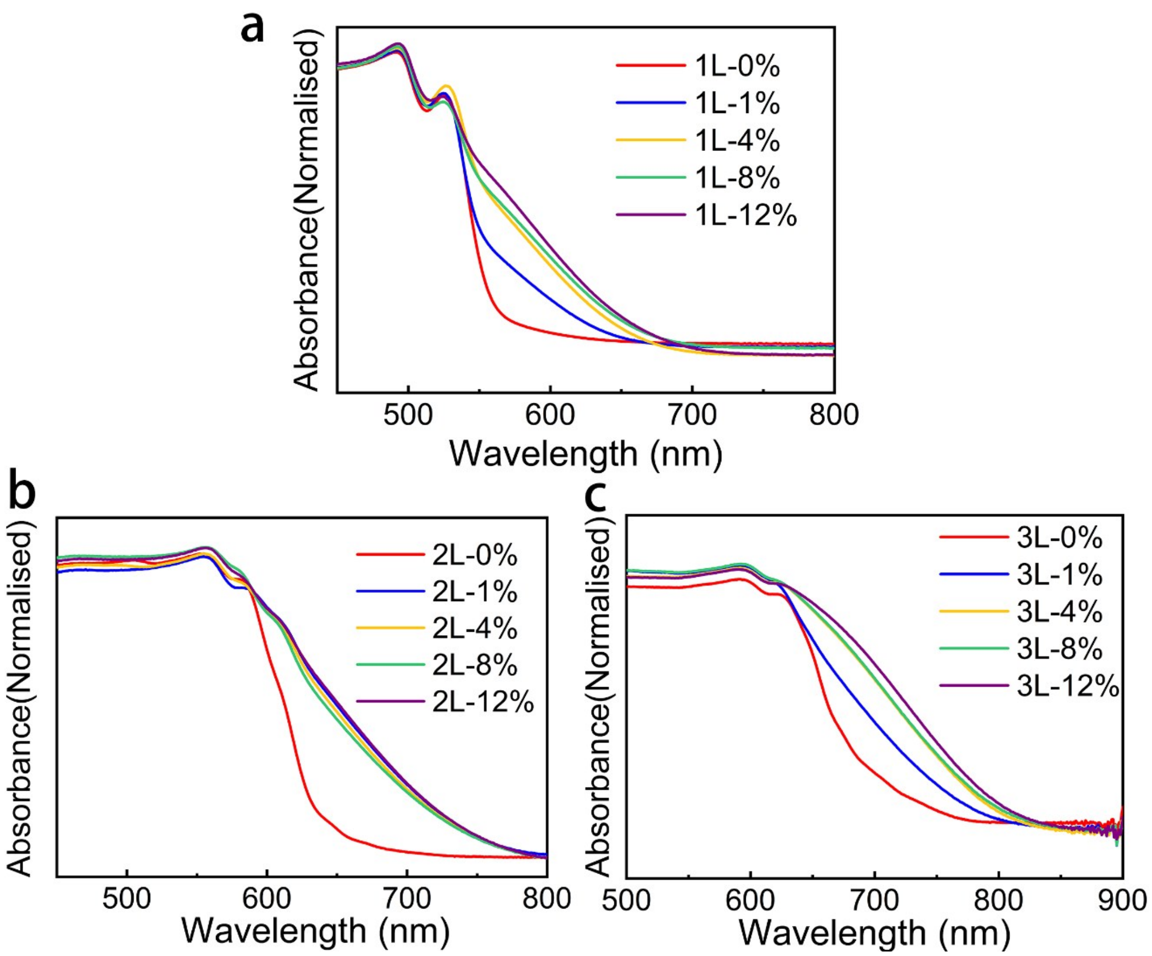

Figure S4. UV-vis absorption spectra of 2D perovskite with various Bi concentration in feed solutions for (a) 1L, (b) 2L & (c) 3L samples.

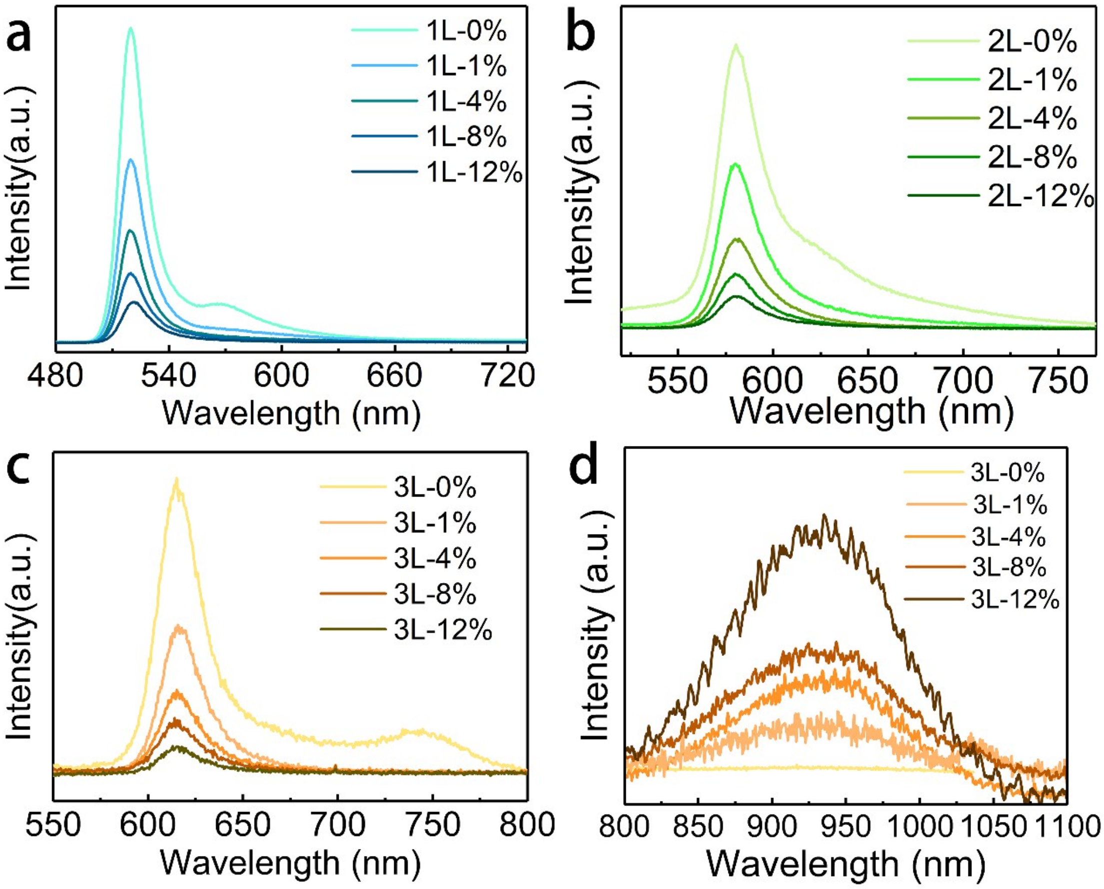

Figure S5. PL spectra of exfoliated crystal samples with various Bi concentration in the feed solution for (a) 1L excitonic PL, (b) 2L excitonic PL, (c) 3L excitonic PL and (d) 3L NIR PL.

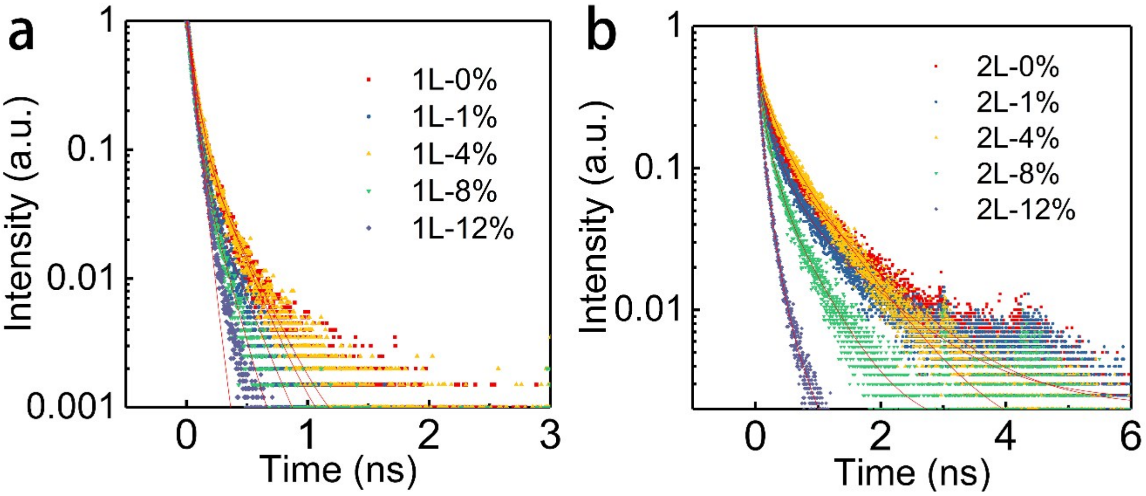

Figure S6. PL decay curves of the exfoliated (a) 1L and (b) 2L 2D RPPs with various Bi concentration in feed solutions.

Table S3. PL lifetime of 1L crystals with various Bi concentration in feed solutions

Bi% in feed solution	τ_1 (ns)	f_1 (%)	τ_2 (ns)	f_2 (%)	τ_{avg} (ns)
0	0.053	83	0.19	17	0.077
1	0.044	90	0.18	10	0.058
4	0.055	88	0.22	12	0.076
8	0.039	85	0.13	15	0.053
12	0.050	100	—	—	0.050

*1L-12% sample can only be fitted by one-exponential model.

Table S4. PL lifetime of 2L crystals with various Bi concentration in feed solutions

Bi% in feed solution	τ_1 (ns)	f_1 (%)	τ_2 (ns)	f_2 (%)	τ_3 (ns)	f_3 (%)	τ_{avg} (ns)
0	0.035	51	0.21	36	0.93	13	0.22
1	0.039	60	0.22	32	0.96	8	0.18
4	0.034	44	0.20	35	0.73	21	0.24
8	0.034	56	0.15	34	0.52	10	0.12
12	0.031	61	0.11	37	0.38	2	0.068

Table S5. PL lifetime of 3L crystals with various Bi concentration in feed solutions

Bi% in feed solution	τ_1 (ns)	f_1 (%)	τ_2 (ns)	f_2 (%)	τ_3 (ns)	f_3 (%)	τ_{avg} (ns)
0	0.026	56	0.58	23	2.5	21	0.68
1	0.023	66	0.31	15	1.6	19	0.37
4	0.027	54	0.19	33	0.83	13	0.18
8	0.027	81	0.21	17	0.72	2	0.073
12	0.018	92	0.20	7	0.18	1	0.033

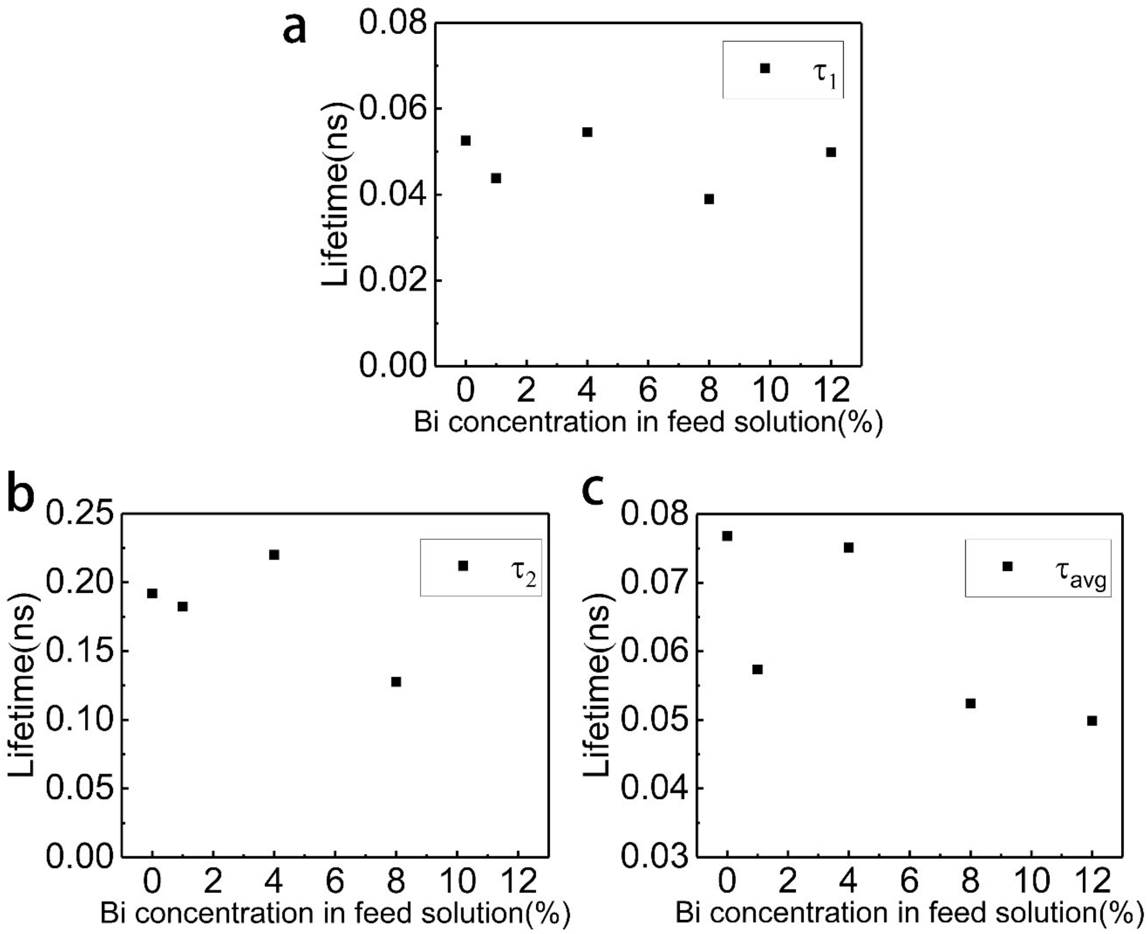

Figure S7. PL lifetime as a function of Bi concentration in the feed solution for 1L samples, (a) τ_1, (b) τ_2, (c) τ_{avg}.

*1L-12% sample can only be fitted by one-exponential model.

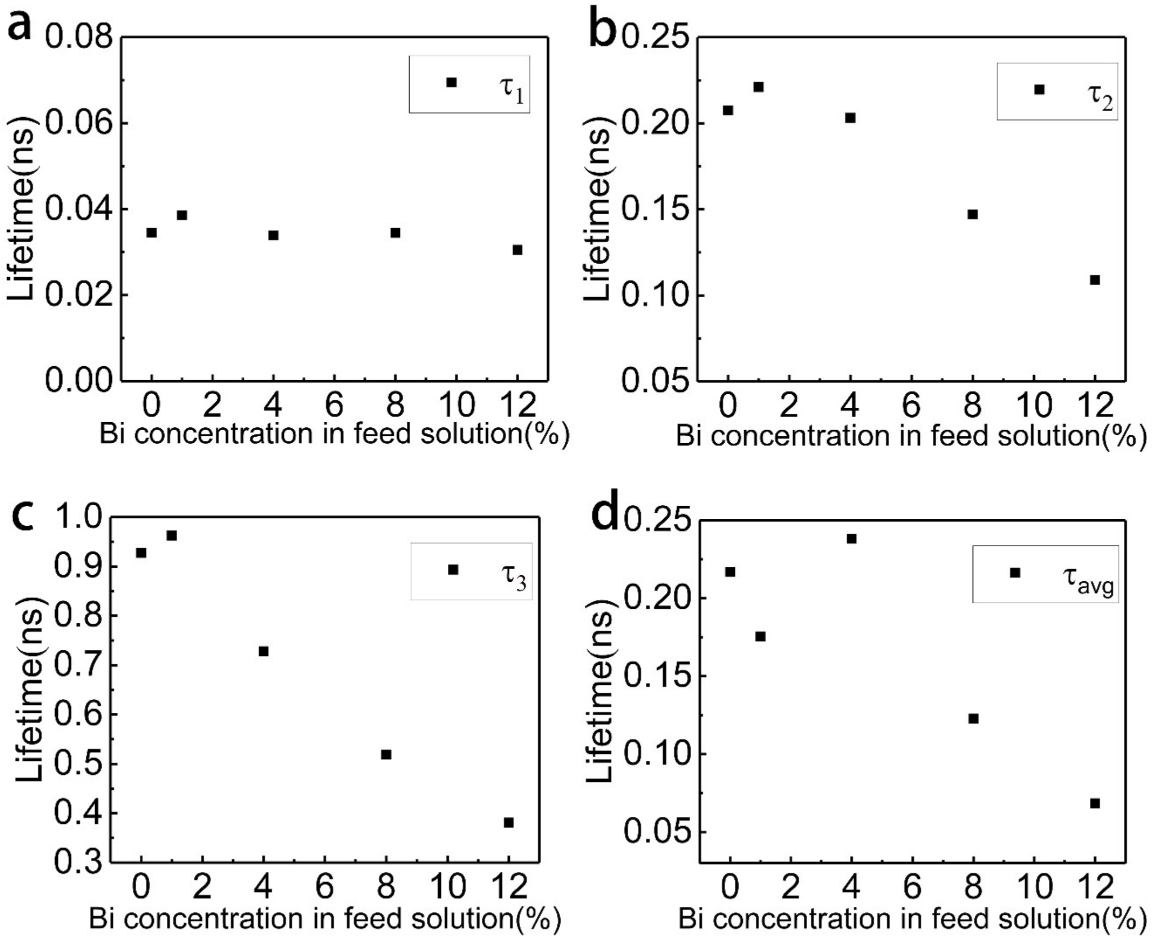

Figure S8. PL lifetime as a function of Bi concentration in the feed solution for 2L samples, (a) τ_1, (b) τ_2, (c) τ_3, (d) τ_{avg}.

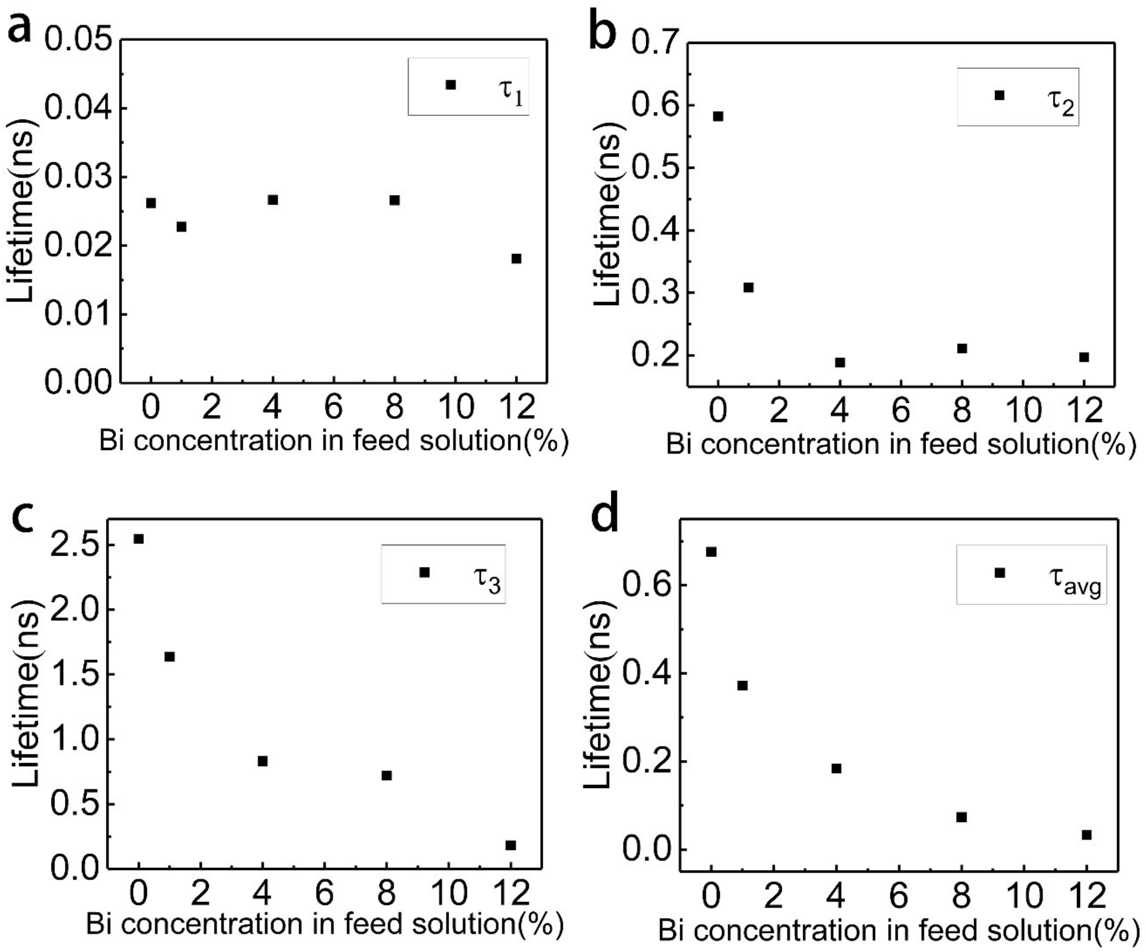

Figure S9. PL lifetime as a function of Bi concentration in the feed solution for 3L samples, (a) τ_1, (b) τ_2, (c) τ_3, (d) τ_{avg}.

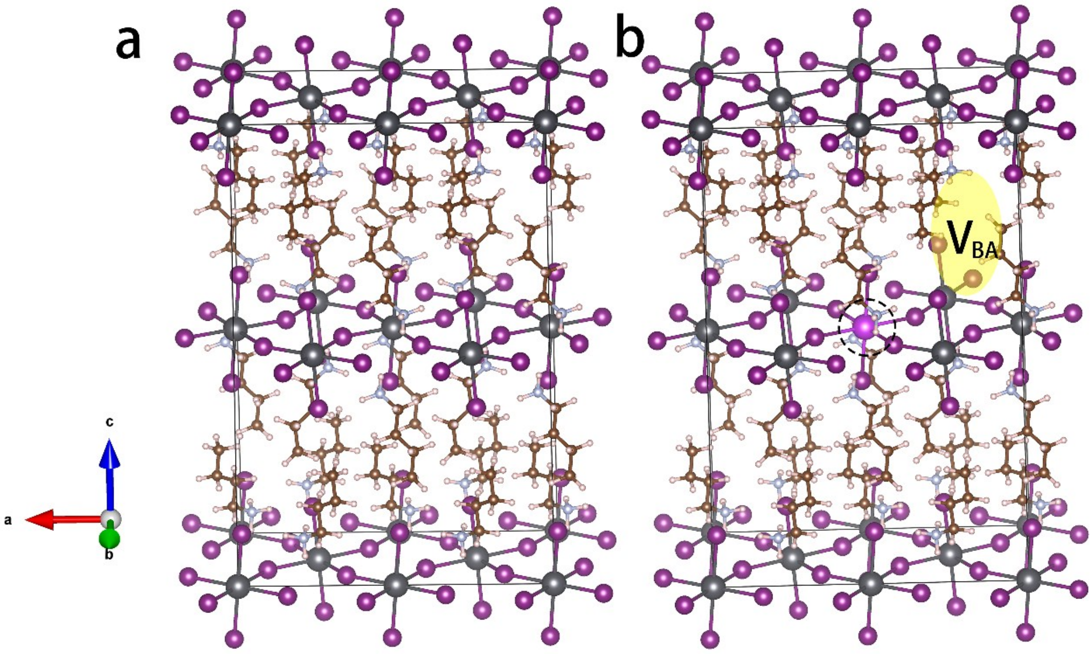

Figure S10. Geometrical structures of (a) $(BA)_2PbI_4$ (1L) and (b) 1L-Bi_{Pb}-V_{BA}

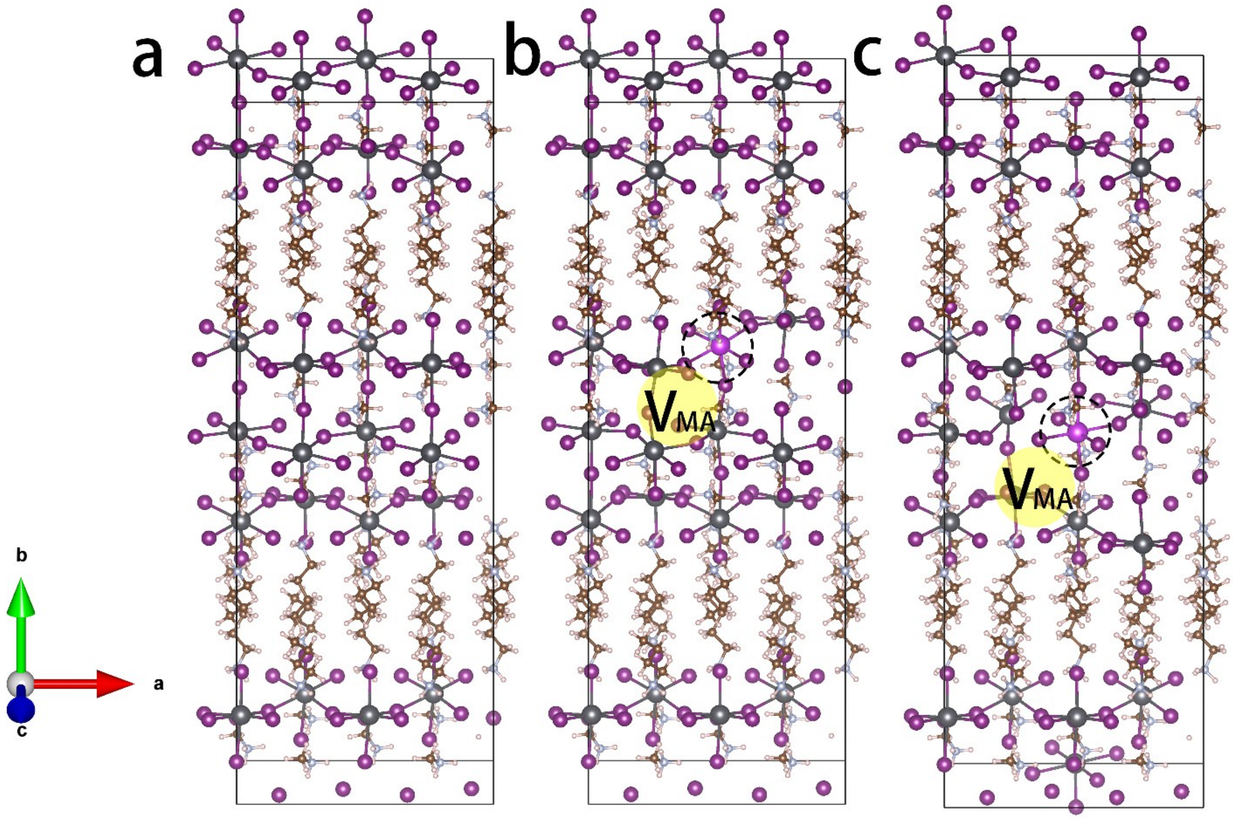

Figure S11. Geometrical structures of (a) $(BA)_2(MA)_2Pb_3I_{10}$ (3L), (b) 3L-$Bi_{top\text{-}Pb}$-V_{MA} and (c) 3L-$Bi_{mid\text{-}Pb}$-V_{MA}.

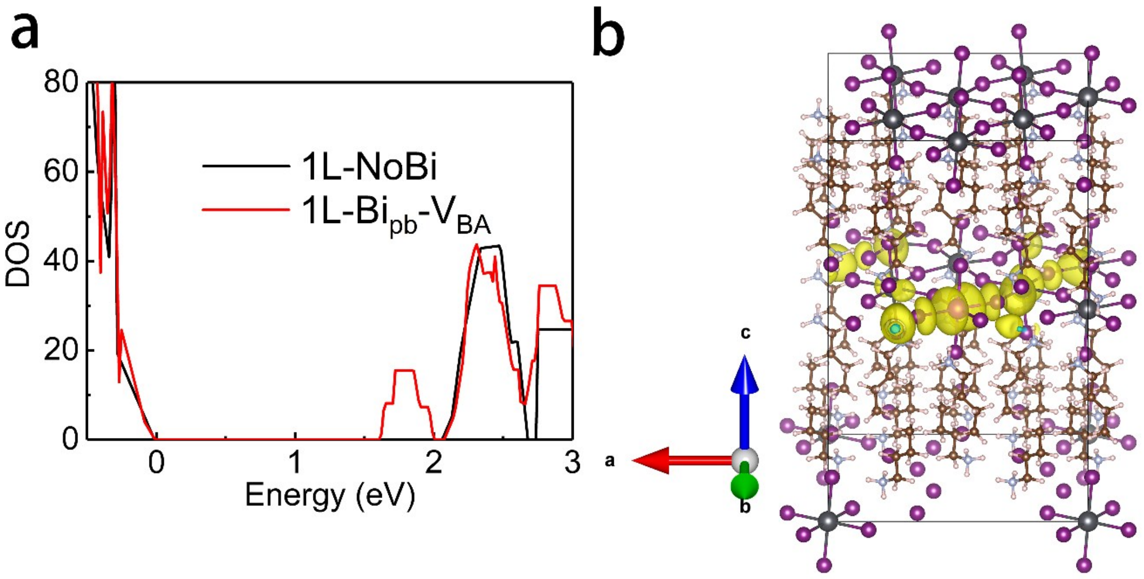

Figure S12. (a) Calculated DOS plots for 1L-2x2x1 system, (b) Partial charge density plot for the CBM of 1L-Bi$_{Pb}$-V$_{BA}$ in 1L-2x2x1 system.

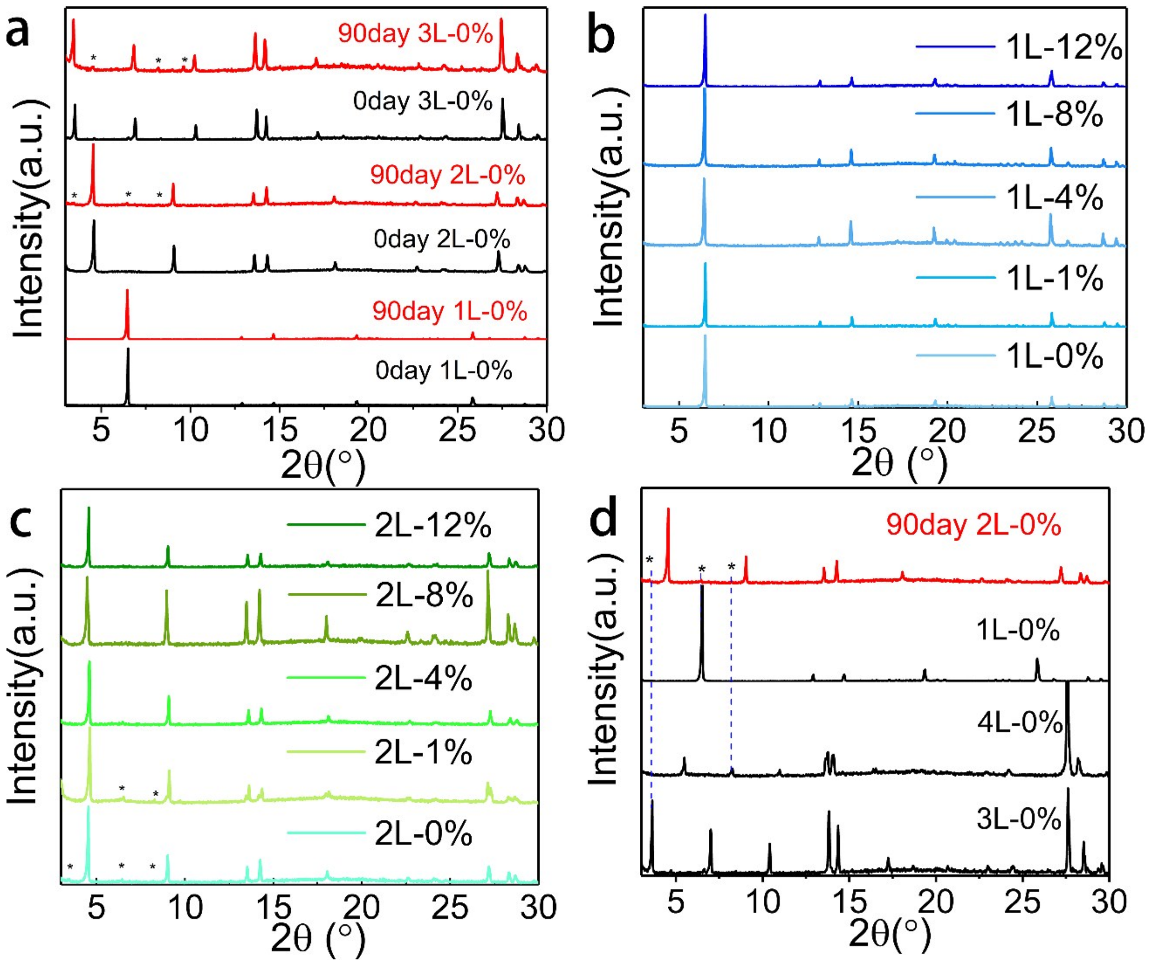

Figure S13. XRD pattern for environmental stability test. (a) undoped samples with n=1,2 & 3 after 90 days, (b) 1L samples with various Bi concentration in feed solutions after 90 days, (c) 2L samples with various Bi concentration in feed solutions after 90 days, (d) 2L-0% after 90 days and fresh 1L-0%, 4L-0% and 3L-0%. The black asterisks highlight the new peaks.

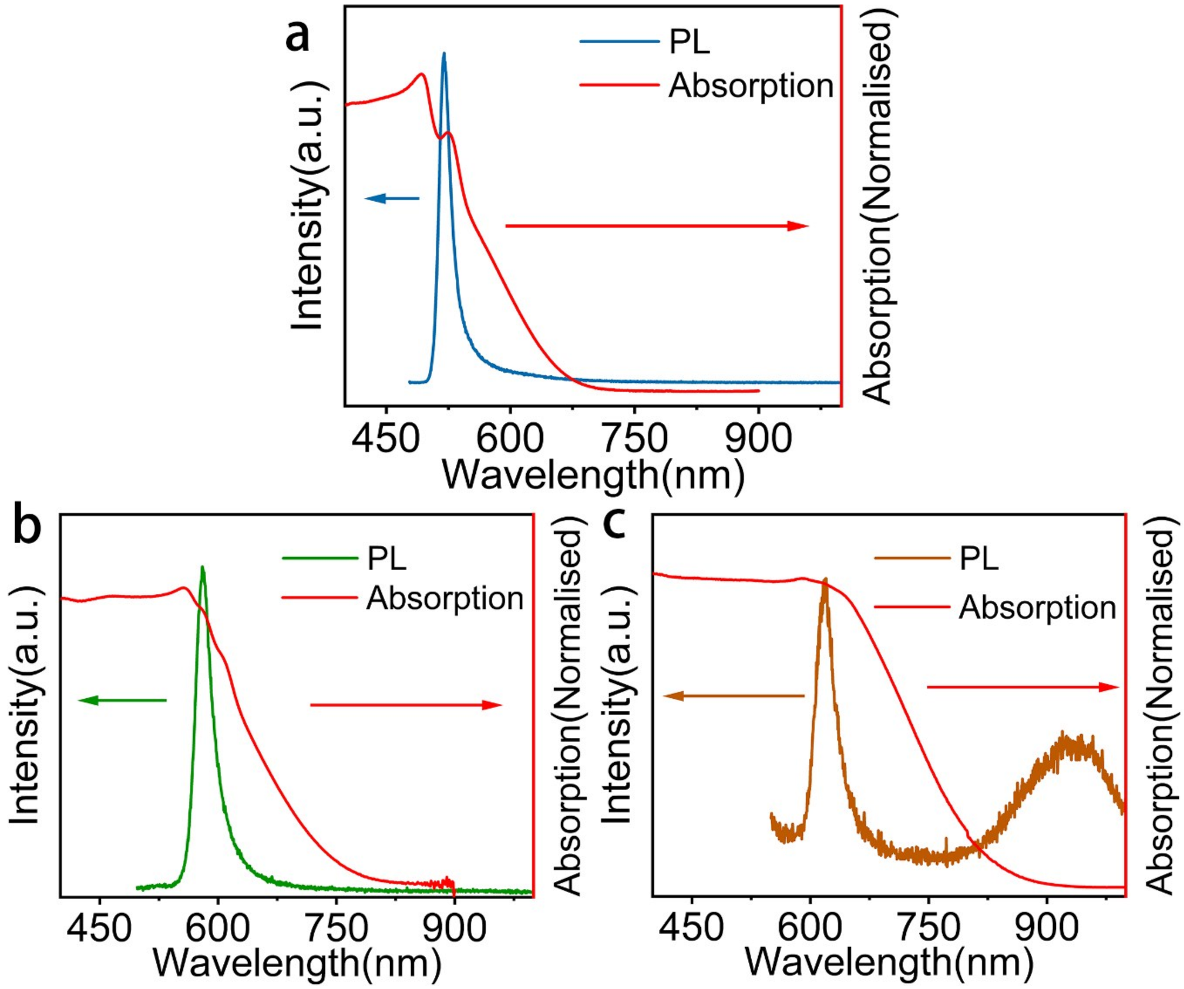

Figure S14. UV-vis absorption and PL spectra for (a) 1L-8%, (b) 2L-8% and (c) 3L-8%.

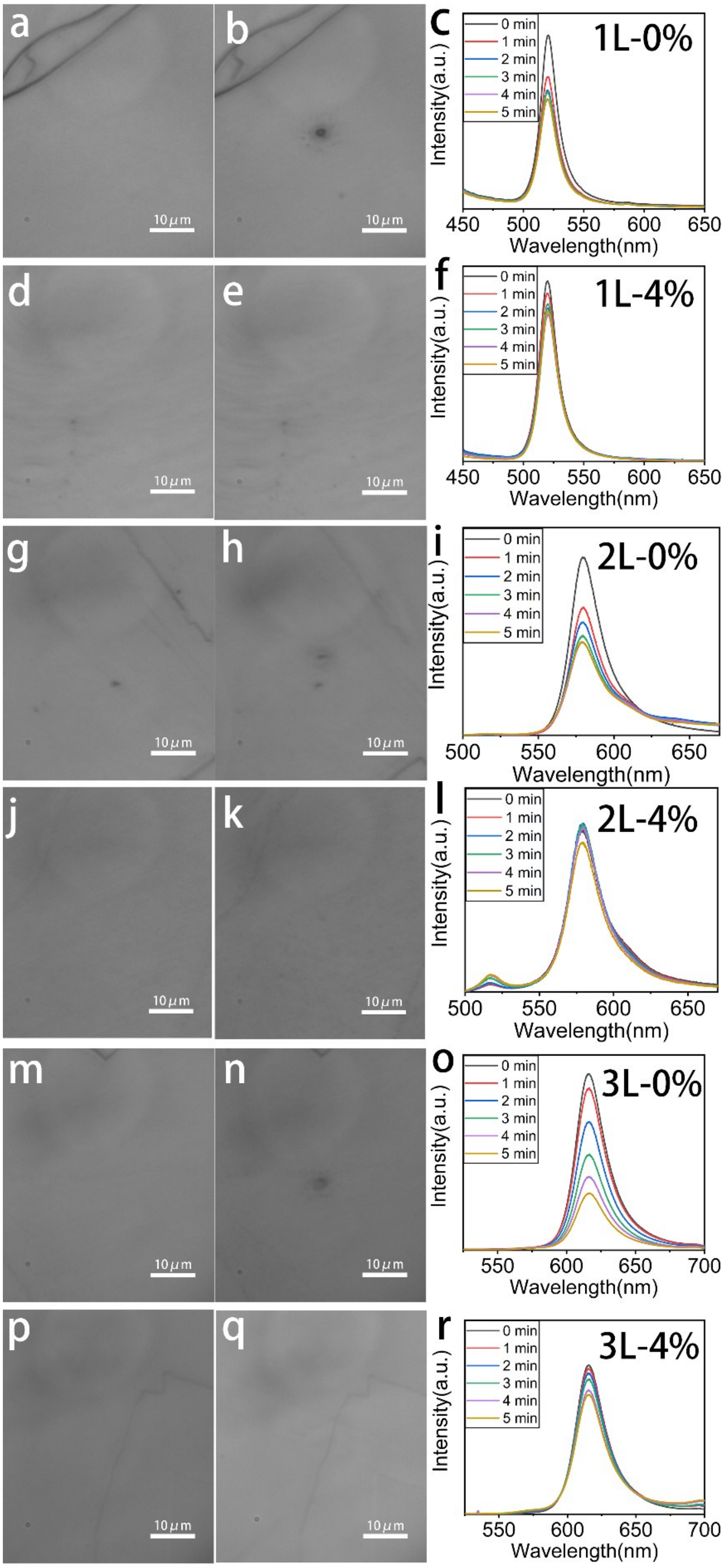

Figure S15. Crystal surface images and PL spectra in photostability tests: (a, d, g, j, m, p) crystals surface before laser exposure for 1L-0%/4%, 2L-0%/4% and 3L-0%/4% respectively; (b, e, h, k, n, q) crystals surface after laser exposure for 1L-0%/4%, 2L-0%/4% and 3L-0%/4% respectively; (c, f, i, l, o, r) PL comparison spectra for 1L-0%/4%, 2L-0%/4% and 3L-0%/4% respectively.

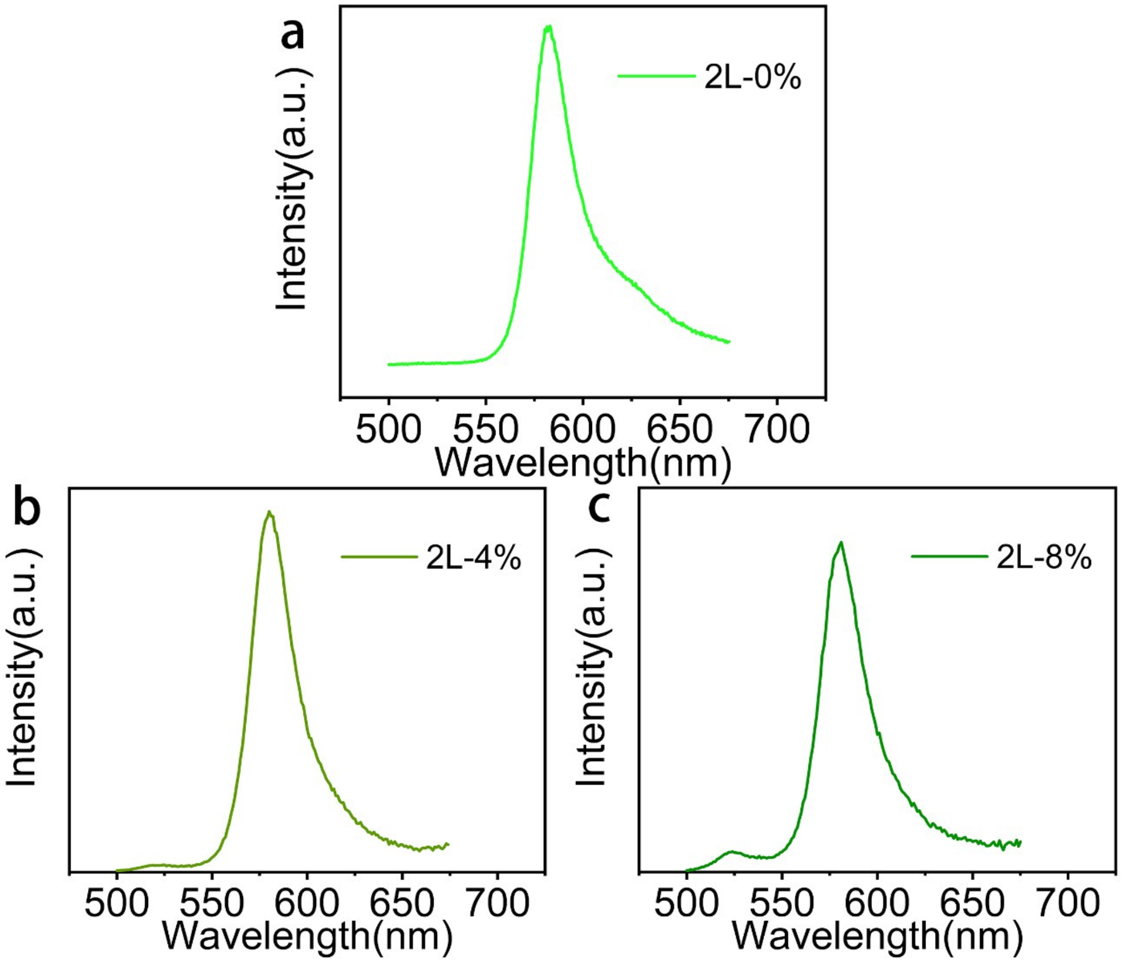

Figure S16. PL spectra for unexfoliated samples: (a) 2L-0%, (b) 2L-4% and (c) 2L-8%.

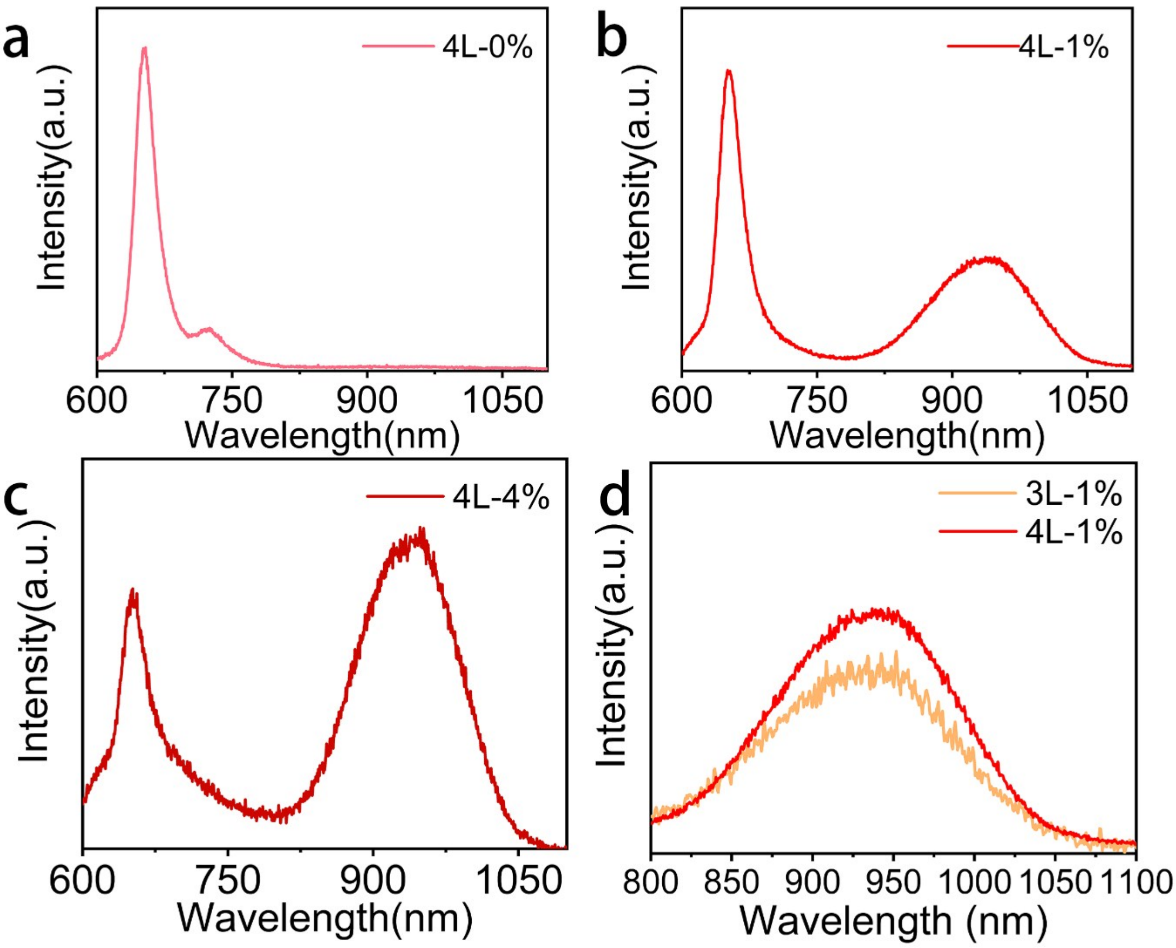

Figure S17. PL spectra for (a) 4L-0%, (b) 4L-1%, (c) 4L-4%, (d) NIR PL for 3L-1% and 4L-1%.

References

1 C. C. Stoumpos, D. H. Cao, D. J. Clark, J. Young, J. M. Rondinelli, J. I. Jang, J. T. Hupp and M. G. Kanatzidis, *Chem. Mater.*, 2016, **28**, 2852-2867.

2 D. G. Billing and A. Lemmerer, *Acta Crystallogr., Sect. B: Struct. Sci., Cryst. Eng. Mater.*, 2007, **63**, 735-747.

3 G. Kresse and J. Furthmuller, *Phys. Rev. B: Condens. Matter Mater. Phys.* , 1996, **54**, 11169-11186.

4 J. P. Perdew, M. Ernzerhof and K. Burke, *J. Chem. Phys.*, 1996, **105**, 9982-9985.

5 J. Klimes, D. R. Bowler and A. Michaelides, *J. Phys.: Condens. Matter.*, 2010, **22**, 022201.